International Journal on Magnetic Particle Imaging
Vol 9, No 1, Suppl 1, Article ID 2303087, 4 Pages

Infinite Science Publishing

Proceedings Article

Passive mixer model for multi-contrast magnetic particle spectroscopy

T. I. Bikulov[a,b,*] · A. Offenhäusser[a,b] · H.- J. Krause[a]

[a]Faculty of Mathematics, Computer Sci. and Natural Sci., RWTH Aachen, 52056 Aachen, Germany
[b]Institute of Biological Information Processing, Forschungszentrum Jülich, 52425 Jülich, Germany
[*]Corresponding author, email: timur.bikulov@rwth-aachen.de

Abstract

For realizing multi-contrast MPI with different types of SuperParamagnetic Nanoparticles (SPN), reconstruction of the particles' core diameter distribution is required for various points in space. We propose a principle for distinguishing signals from SPNs of different diameters, which exploits the offset field concept already used in MPI. We show that precise reconstruction of Magnetization Curve (MC) is the key to precise reconstruction of core diameter distribution, as all information about distribution is stored in the curvature. A Passive Mixer Model is proposed in order to uniquely relate the MC to the intermodulation products in the magnetization spectra. The model does not require small signal assumption and hence does not lose accuracy in the reconstruction under large excitation fields. We show that a number of useful practical conclusions can be drawn from this model.

I. Introduction

The natural evolution of any contrast-based imaging technique is ability to simultaneously detect several target analytes. Probing the nonlinearity of the magnetization curve (MC) of superparamagnetic nanoparticles (SPN) with magnetic particle spectroscopy (MPS) or frequency mixing magnetic detection (FMMD) [4,5] allows to extract concentration information (from amplitude) and binding information (from phase) of several superparamagnetic nanoparticle (SPN) species, opening up new opportunities for multi-target magnetic immunoassays. We report a principle that exploits the non-linear properties and asymptotic nature of MC to separate signals from SPNs of different core size diameters. A similar principle is utilized in Multi-Harmonic Atomic Force Microscopy to distinguish between magnetic and non-magnetic forces contribution of cantilever-sample interaction [1]. We show that the key for multi-contrast MPI measurement consists in precise reconstruction of the MC. As further elaboration, a Passive Mixer Model (PMM) is introduced. This model reduces the inverse problem of MC reconstruction to system of linear equations. PMM allows to bypass the small signal assumption that is usually done in analysis of nonlinear distortions [2,4].

II. Signal Separation Principle

The statistical expectancy $E\{\cdot\}$ of the SPN sample magnetic moment $m(B)$ [Am^2] depends on field B [T] can be calculated by

$$E\{m(B)\} = \frac{\pi}{6} N_p M_s \int_0^{\infty} d_c^3 \mathscr{L}\left(\frac{\pi}{6}\frac{M_s d_c^3}{k_B T} B\right)\rho_d(d_c)\, d\, d_c \tag{1}$$

Where N_p is number of particles, $\rho_d(d_c)$ is probability density function of particle magnetic core diameter d_c [m], M_s [A/m] is volumetric magnetization, $\mathscr{L}$(x)=coth$(x) - 1/x$. Let's assume two monodisperse samples of SPNs of 7 nm and 15 nm. Their normalized

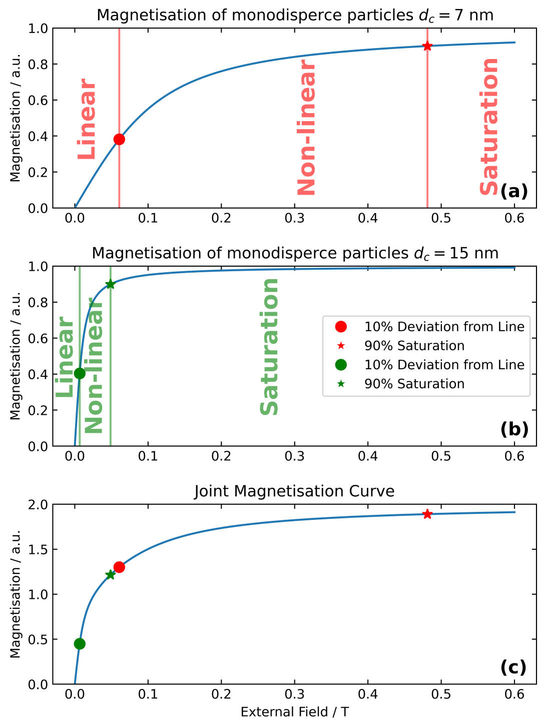

Figure 1: Principle of signal separation from SPNs with different core diameters

MCs are depicted in Fig. 1 (a) and (b), respectively.

Conventionally one can divide these curves into three regions: the linear, non-linear and saturation. If excitation signal stays in the linear region, no Non-Linear Harmonics (NLH, i.e., higher order fundamental harmonics and intermodulation products) occur, but the amplitude of the Fundamental Harmonic (FH) is affected. In contrast, in the saturation region, FH is suppressed, but NLH are not produced as well. In the non-linear region, NLH appear. These regions have a pairwise independent influence on the signal. In practice, the amplitude of the excitation field is limited from below by the SNR of the measurement system. The resulting MC is a linear superposition of the initial ones, see Fig. 1 (c). The non-linear region of larger SPN overlaps with the linear region of smaller SPN. In the non-linear region of smaller SPN, larger SPN are already saturated. As the number of SPN of each type changes, their contribution will change proportionally. By analysing the asymptotes of the Langevin curve, it can be shown that the approximate position of the nonlinearity region of monodisperse particles can be calculated by the formula

$$B_n(d_c) = \frac{6k_B T}{\pi d_c^3 M_s}\sqrt[4]{15} \tag{2}$$

When measured close to B_n, particles of d_c diameter make the greatest contribution to non-linearity. By choosing initial SPN with distant B_n values and by accurately reconstructing the MC, it is possible to independently extract information about the concentration of each individual particle type. The technical feasibility of independent concentration measurement of two particle species mixture by measurement of nonlinear distortions has been already demonstrated in our group [5].

III. Passive Mixer Model

For precise reconstruction of the MC, a model that relates the MC shape to the amplitudes of the FH and NLHs in magnetization spectra is required. As the range of applicable magnetic fields $[-B_{max}, B_{max}]$ is practically limited by the field generator and the MC is always odd and monotonously increase one can uniquely approximate it with Chebyshev polynomials $T_n(x)$ of L terms.

$$\hat{m}(B) = \sum_{i=0}^{L-1} a_i T_{2i+1}(B) \tag{3}$$

Let's assume that excitation field consist of dc offset B_0 and a couple of harmonic oscillators: B_1 and B_2. Such definition covers most of ac-susceptometry based techniques such as MPI, two-harmonic MPI, MPS and FMMD.

$$B(t) = B_0 + B_1 sin(2\pi f_1 t + \theta_1) + B_2 sin(2\pi f_2 t + \theta_2) \tag{4}$$

Assume that the particles respond to the external field fast enough i.e. the effective relaxation time τ_{eff} is small enough: $\tau_{eff} \ll \min(f_1{}^{-1}, f_2{}^{-1})$. By substituting $B(t)$ into (3) and applying the multinomial expansion, one can obtain general expression for magnetization signal in terms of spectral line sum.

$$\hat{m}(t) = \sum_{i=0}^{L-1} a_i \frac{2i+1}{2} \sum_{r=0}^{i} (-1)^r \frac{(2i-r)!}{r!} B_{max}^{-(2i-2r+1)} \cdot \sum_{\sum_{l=1}^{5} k_l = 2i+1}^{n} \frac{(2i+1)!}{\prod_{m=1}^{5} k_m!} 2^{k_5} B_0^{k_5} B_1^{k_1+k_2} B_2^{k_3+k_4} P(\vec{k}) F(\vec{k}, t) \tag{5}$$

$$P(\vec{k}) = exp(i(\varphi_1(k_1 - k_2) + \varphi_2(k_3 - k_4))) \tag{6}$$

$$F(\vec{k}, t) = exp(i2\pi t(f_1(k_1 - k_2) + f_2(k_3 - k_4))) \tag{7}$$

Using (5) it is possible to obtain a polynomial expression for an arbitrary harmonic $f_t = bf_1 + cf_2$ for $\forall b, c \in \mathbb{Z}$. To do that one should solve the subset-sum problem for each i^{th} polynomial coefficient by calculating a set S_i of

k-vectors that fulfil:

$$S_i(b,c)=\left\{\overrightarrow{k}\,|k_1,k_2,\ldots,k_5\in\mathbb{Z}\geq 0\wedge k_1-k_2=b\wedge k_3 -k_4=c\wedge\sum_{l=1}^{5}k_l=2i+1\right\} \tag{8}$$

The subset sum problem can be solved by dynamic programming methods by iterating over the elements of a unidirectional tree. In this way, only those elements that contribute to the frequency f_t. are selected from the general sum. Then the measurement vector $\overrightarrow{v}$ can be calculated.

$$\overrightarrow{v}(B_0,B_1,B_2,b,c)=\left(v_i|v_i=\frac{2i+1}{2}\sum_{r=0}^{i}(-1)^r\frac{(2i-r)!}{r!} B_{max}^{-(2i-2r+1)}\cdot\sum_{\overrightarrow{k}\in S_i(b,c)}\frac{(2i+1)!}{\prod_{m=1}^{5}k_m!} 2^{k_5}B_0^{k_5}B_1^{k_1+k_2}B_2^{k_3+k_4}\right) \tag{9}$$

Finally, the amplitude $A_{bf_1+cf_2}$ of f_t harmonic in magnetization signal can be calculated by a scalar product:

$$\overrightarrow{v}(\overrightarrow{p})\cdot\overrightarrow{a}=A_{bf_1+cf_2} \tag{10}$$

where $\overrightarrow{a}=(a_i|i\in\{0,1,\ldots,L-1\})$ is a vector that consists of polynomial approximation coefficients and $\overrightarrow{p}=(B_0,B_1,B_2,b,c)$ is a vector in measurement parameter space. In a real measurement system, some recordings might be taken simultaneously, e.g., measurement of f_1, $3f_1$ and $5f_1$ in MPS, or of $f_1\pm 2f_2$, $f_1\pm 3f_2$, ... in FMMD. For a measurement process that consists of a set $D=\{\overrightarrow{p}_i|i\in\{0,1,\ldots N\}\}$ of N recordings, the measurement can be expressed as a system of linear equations. MC reconstruction turns into a well investigated linear inverse problem. E.g., for simultaneous MPS measurement of f_1, $3f_1$ and $5f_1$, such a matrix for single measurement point looks as:

$$\begin{pmatrix} v_0(\overrightarrow{p_1}) & v_1(\overrightarrow{p_1}) & v_2(\overrightarrow{p_1}) & \ldots & v_{L-1}(\overrightarrow{p_1})\\ 0 & v_1(\overrightarrow{p_3}) & v_2(\overrightarrow{p_3}) & \ldots & v_{L-1}(\overrightarrow{p_3})\\ 0 & 0 & v_2(\overrightarrow{p_5}) & \ldots & v_{L-1}(\overrightarrow{p_5})\end{pmatrix}\begin{pmatrix}a_0\\ a_1\\ \vdots\\ a_{L-1}\end{pmatrix}=\begin{pmatrix}A_{f_1}\\ A_{3f_1}\\ A_{5f_1}\end{pmatrix} \tag{11}$$

IV. Numerical Simulation

To demonstrate the effectiveness of the approach, a numerical simulation of 0D MPS signal acquisition was performed. A binary mixture of SPN was defined by a probability mass function (Fig. 2) with parameters given in Table 1. The MC for the mixture was calculated by using (1). Excitation signal was calculated with time step of 5 µs. Only $f_1=1$ kHz was applied with amplitude $B_1=10$ mT. The dc offset component B_0 varied from 0 to 100 mT in steps of 1 mT. For each point of excitation signal in Time Domain (TD), the value of MC was interpolated. The magnetization signal was digitally demodulated at f_1, $3f_1$ and $5f_1$ and averaged over 1 second of simulation time.

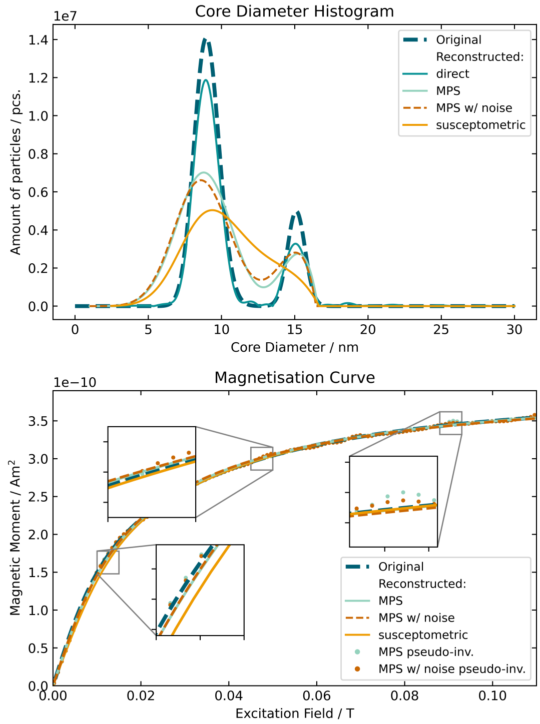

Figure 2: Numerical investigation of reconstruction performance

At first, the distribution from the original MC was reconstructed to evaluate the information loss due to reconstruction process ("direct"). Then the MC was reconstructed using PMM out of MPS TD simulation data, once without noise ("MPS") and once with noise ("MPS w/ noise"). The number of polynomial coefficients was selected to $L=16$. Total number of rows in measurement matrix was 300. The reconstruction range was $B_{max}=\max(B_0+B_1)=110$ mT. The MC was reconstructed by 5 step procedure in which B_{max} was linearly increased and pseudo-inverse matrix was calculated. This procedure is necessary to maintain the density of Chebyshev approximation points as they are denser at the edges and therefore reconstruction is more precise. On each iteration the reconstructed MC points for larger field values were appended to previous ones. In Figure 2, the raw reconstructed MC points are shown as dots. At the joints of the segments (Figure 2, top and right insets) the discrepancies can be seen. In contrast to "MPS", reconstruction "MPS w/ noise" was conducted with addition of gaussian noise applied in TD with zero mean and standard deviation of $\sigma=3.2\cdot 10^{-10}$ Am^2 to imitate a noisy environment. Finally, the susceptometry signal at

10.18416/ijmpi.2023.2303087

Table 1: Parameters of original core diameter distribution.

	Amount	Mean	FWHM
Sample 1	10^9 pcs.	9 nm	2 nm
Sample 2	$25{\cdot}10^7$ pcs.	15 nm	1.4 nm

frequency f_1 of TD simulation was integrated to reconstruct the MC in a conventional way ("susceptometric") and obtain the distribution.

The core diameter distribution is reconstructed using Non-Negative Least Squares approach with regularization [2] by approximating (1) with a sum. In case of "direct" reconstruction, the regularization parameter was $\lambda_1 = 10^{-7}$, obtained by minimizing the error between original and reconstructed distribution to show the performance limit of the reconstruction algorithm. For "MPS" and "MPS w/ noise" reconstructions, the parameter $\lambda_2 = 3 \cdot 10^{-4}$ was obtained considering the amount and position of extrema in solution.

V. Results and discussion

PMM (Eqs. 5-7) allows a number of useful conclusions to be drawn under assumption of small effective relaxation time τ_{eff}: a) the NLH amplitude (10) is independent of the excitation field phases $\theta_{f_1}, \theta_{f_2}$. b) The phase of any NLH (6) is a linear combination of phases of excitation fields: $\theta_{bf_1 \pm cf_2} = b\theta_{f_1} \pm c\theta_{f_2}$. c) NLH amplitudes are symmetric around FH $f_1$and f_2: $A_{bf_1+cf_2} = A_{bf_1-cf_2}$. d) The higher the order $|b|+|c|$ of NLH, the less information it contains about the magnetization curve. e) The more NLH are simultaneously measured, the more orthogonal components are available. f) For MC reconstruction, at least one measurement of FH should be conducted (all Eq. (11)). Otherwise, the information about absolute amount of SPN (scaling factor) is lost, but information about relative amounts is still preserved. In more general case, PMM is not valid, as for large relaxation time $\tau_{eff} > \min\left(f_1^{-1}, f_1^{-2}\right)$, it becomes field-dependent $\tau_{eff} = \tau_{eff}(B_0, B_1, B_2)$ [3].

Numerical simulation shows that for large realistic FH amplitude and SPN core diameters, the conventional susceptometry loses the information just at the place with the highest non-linearity, where the information about the SPN core diameters is retained (Fig. 2, left bottom inset).

That results in smearing of the distribution and inability to reconstruct particle concentrations separately. With all other parameters unchanged, additional measurement of $3f_1$ and $5f_1$ components allowed recovering missing information by using PMM.

VI. Conclusions

PMM revealed a number of NLH properties and also made it possible to circumvent the small-signal approximation, which in practice did not allow large amplitudes to be used to achieve high SNR without losing reconstruction precision. The next step is to determine the optimum measurement scheme to extract the most complete information about MC. In the future, the PMM and its reconstruction principles could be used to solve the inverse problem for realizing a multi-contrast MPI system.

Acknowledgments

Research funding from German Federal Ministry of Food and Agriculture (BMEL), contract 2818710C19 is gratefully acknowledged.

Author's statement

Conflict of interest: Authors state no conflict of interest.

References

[1] D. Forchheimer et al., *Simultaneous imaging of surface and magnetic forces*, Applied Physics Letters, vol. 103, Jul. 2013.

[2] Y. Sun et al., *An Improved Method for Estimating Core Size Distributions of Magnetic Nanoparticles via Magnetization Harmonics*, Nanomaterials, vol. *10*(9), pp.1623-1635, Aug. 2020.

[3] M. I. Shliomis, *On the kinetics of magnetization of suspension of ferromagnetic particles*, Soviet Physics-JETP, vol. 38(2), pp.413-416, Feb. 1974

[4] H. J. Krause et al., *Magnetic particle detection by frequency mixing for immunoassay applications*, J. Magn. Magn. Mater., vol. 311(1), pp.436-444, Dec. 2007

[5] A.M. Pourshahidi et al., Multiplex Detection of Magnetic Beads Using Offset Field Dependent Frequency Mixing Magnetic Detection, Sensors, vol. 21(17), pp. 5859, Aug. 2021

10.18416/ijmpi.2023.2303087